Acta Chemica Scandinavica, 1997: 51: 1241–1244
Printed in UK – all rights reserved

ACTA
CHEMICA SCANDINAVICA
ISSN 0904-213X

Hamigerone and Dihydrohamigerone: Two Acetate-Derived, Antifungal Metabolites from *Hamigera avellanea*

Jens Breinholt,[a,*] Anders Kjœr,[b] Carl E. Olsen,[c] Birgitte R. Rassing[a] and Connie N. Rosendahl[a]

[a]Novo Nordisk A/S, DK-2880, Bagsvœrd, Denmark, [b]Department of Organic Chemistry, The Technical University of Denmark, DK-2800 Lyngby, Denmark and [c]Chemistry Department, The Royal Veterinary and Agricultural University, DK-1871 Frederiksberg C, Denmark

Breinholt, J., Kjœr, A., Olsen C. E., Rassing, B. R. and Rosendahl, C. N. 1997. Hamigerone and Dihydrohamigerone: Two Acetate-Derived, Antifungal Metabolites from *Hamigera avellanea*. – Acta Chem. Scand. 51: 1241–1244. © Acta Chemica Scandinavica 1997.

The fungus *Hamigera avellanea* is found to be the source of two metabolites, hamigerone ($C_{25}H_{32}O_5$) and dihydrohamigerone ($C_{25}H_{34}O_5$), the former exhibiting *in vitro* growth inhibitory activity against phytopathogenic fungi. Their chemical structures and configurations, save for details related to the stereochemistry, have been established by a variety of spectroscopic techniques. Feeding the fungus with specifically labelled ^{13}C-precursors served to establish the biosynthetic derivation of the two metabolites from ten intact acetate and five methionine-derived C_1-units.

During a search for fungal metabolites inhibiting the growth of the rice blast fungus *Pyricularia oryzae* we became aware of the inhibitory effect displayed by culture filtrates of the fungus *Hamigera avellanea* (Ascomycota). Bioassay-guided fractionation afforded two structurally related metabolites, *hamigerone* and *dihydrohamigerone*, the former of which is responsible for the observed inhibitory activity. We report on the structure elucidation, biosynthesis, and biological properties of the two metabolites.

Structure elucidation

Hamigerone and dihydrohamigerone were isolated from fermentations of *Hamigera avellanea* as described in Experimental.

Hamigerone. This major metabolite was obtained as a homogeneous, amorphous, colourless, and moderately stable solid, exhibiting an HR-FAB mass spectrum in accordance with the molecular composition $C_{25}H_{32}O_5$, with an index of hydrogen deficiency of 10. Its ^1H NMR spectrum, recorded in deuteriobenzene, displayed signals corresponding to 31 non-exchangeable protons, whereas 25 magnetically non-equivalent nuclei were observable in the ^{13}C NMR spectrum (Table 1). DEPT spectra established these as attributable to six methyl, two methylene, five methines (one oxygenated), one (oxygenated) quaternary, eight alkenic, one carboxy, and two ketonic carbon atoms. Consequently, hamigerone must contain three ring units. ^1H and ^{13}C NMR data (Table 1), supplemented with 2D NMR measurements (COSYPHDQ, TOCSY, HSQC, HSQC-TOCSY, and HMBC), enabled us to identify a number of structural elements and combine them to give structure **1**.

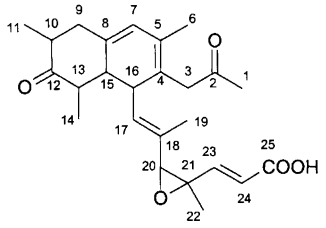

1

Facile conversion of hamigerone into its methyl ester upon reaction with diazomethane, intensive IR keto-absorption at 1707 cm^{-1}, and a large $^1H,^{13}C$ coupling constant (176 Hz), observed for C-20 and characteristic of hydrogen-carrying oxirane carbon atoms, are all features in accordance with structure **1**. The UV spectrum of hamigerone exhibited an intense absorption band at ca. 280 nm in good agreement with its character as a pentaalkylated homoannular diene. The long-range $^1H,^{13}C$-correlations established are shown in Fig. 1.

* To whom correspondence should be addressed.

Table 1. ^1H and ^{13}C NMR data for hamigerone (**1**) in C_6D_6 and dihydrohamigerone (**3**) in $CDCl_3$.

	1		**3**	
C	1H[a]	^{13}C	^1H[b]	^{13}C
1	1.75 (s)	28.97 (q)	1.33 (d)	24.07 (q)
2		204.37 (s)	4.60 (dq)	64.35 (d)
3	3.12 (d)	46.52 (t)	5.62 (d)	131.2 (d)
3′	2.60 (d)			
4		122.96 (s)		136.00 (s)
5		127.26 (s)		132.83 (s)
6	1.55 (s)	18.11 (q)	1.91 (s)	19.95 (q)
7	5.40 (s)	122.45 (d)	5.65 (s)	131.3 (d)
8		138.21 (s)	2.77 (br s)	32.39 (d)
9	2.23 (dd)	42.44 (t)	2.10 (ddd)	40.84 (t)
9′	1.66 (dd)		1.60 (dt)	
10	1.90 (m)	48.51 (d)	2.49 (m)	41.03 (d)
11	1.06 (d)	15.21 (q)	1.00 (d)	14.43 (q)
12		210.03 (s)		214.04 (s)
13	2.26 (dq)	49.21 (d)	2.32 (dq)	43.81 (d)
14	1.26 (d)	11.28 (q)	1.08 (d)	11.43 (q)
15	1.64 (d)	49.93 (d)	1.74 (m)	50.28 (d)
16	3.19 (d)	38.22 (d)	3.79 (dd)	36.91 (d)
17	5.52 (d)	129.21 (d)	5.49 (d)	128.73 (d)
18		128.54 (s)		128.73 (s)
19	1.50 (s)	14.17 (q)	1.78 (s)	14.02 (q)
20	3.00 (s)	67.73 (d)[c]	3.30 (s)	67.64 (d)[d]
21		60.32 (s)		60.66 (s)
22	1.02 (s)	13.75 (q)	1.29 (s)	13.92 (q)
23	6.95 (d)	151.49 (d)	6.90 (d)	151.53 (d)
24	6.14 (d)	121.87 (d)	6.05 (d)	120.47 (d)
25		170.73 (s)		168.66 (s)

[a] *J*-values: $J_{3,3'}=14.6$, $J_{9,9'}=11.6$, $J_{9,10}=6.3$, $J_{9',10}=12$, $J_{10,11}=6.4$, $J_{13,14}=6.4$, $J_{13,15}=12$, $J_{15,16}\sim 0$, $J_{16,17}=10.6$, $J_{23,24}=15.6$. [b] *J*-values: $J_{1,2}=6.0$, $J_{2,3}=8.0$, $J_{8,9}=2.3$, $J_{8,9'}=4.9$, $J_{8,15}$, not determined, $J_{9,9'}=13.3$, $J_{9,10}=5.1$, $J_{9',10}=13.5$, $J_{10,11}=6.4$, $J_{13,14}=6.4$, $J_{13,15}=12$, $J_{15,16}=2.7$, $J_{16,17}=9.2$, $J_{23,24}=15.6$. [c] $^1J_{CH}=176$. [d] $^1J_{CH}=174$.

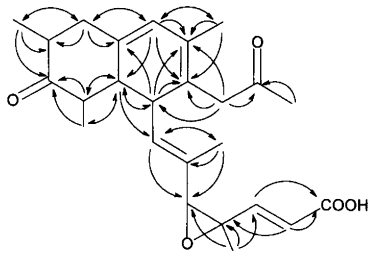

Fig. 1. Long-range $^1H,^{13}C$ correlations established in the HMBC-spectrum of hamigerone (**1**).

To clarify the ring stereochemistry, vicinal coupling constants ($^3J_{HH}$) and NOE-interactions (1D-NOE differences and/or 2D-NOESY measurements, at 600 MHz) were invoked. They served to establish (i) that H-10 and H-13 occupy *cis* axial positions ($^3J_{9',10}=^3J_{13,15}=12$ Hz; strong H-10/H-13 transannular NOE interaction); (ii) that H-9′ and H-15 constitute another, *trans*-positioned, *cis*-axial, proton pair (the coupling constants quoted, supplemented with NOESY correlation between the equatorial H-9 and H-7); and (iii) that H-16 in the planar diene ring is located '*trans*' to the axial H-15 ($^3J_{15,16}\sim 0$; strong NOE between H-15 and H-17). Consequently, the bicyclic moiety of hamigerone is represented by structure **2** (or its mirror image). By the same means it was established that in the side-chain, R, *E*-configurations prevail around the C-23/C-24 ($^3J_{23,24}=15.6$ Hz) and C-17/C-18 (NOE from H-17 to H-20) double bonds. NOE interactions between H-20 and H-23, as well as H-24, but not H-22, served to verify the *trans*-relationship of the C-22 methyl group and H-20. The question of whether the side-chain is correctly represented by the structure shown (20*R*,21*R*), or rather by its mirror image (20*S*,21*S*), remains unanswered.

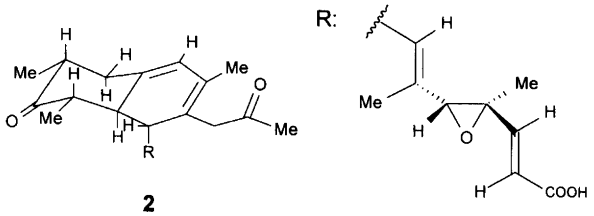

2

Dihydrohamigerone. Dihydrohamigerone, the minor congener of hamigerone, was obtained, virtually homogeneous, as a rather unstable, amorphous, colourless solid. HR-FAB mass spectrometry revealed its molecular composition as $C_{25}H_{34}O_5$. The ^1H and ^{13}C NMR spectra (Table 1), supplemented with the same array of 1-D and 2-D NMR techniques that were utilised in the structure elucidation of hamigerone, indicated that dihydrohamigerone possesses the skeletal structure **3**, supported by its UV spectrum with λ_{max} at ca. 240 nm, the expected value for a tetrasubstituted heteroannular diene. Obviously, the formal reduction of the 2-oxo group of hamigerone (**1**) to the carbinol function of its dihydroanalogue (**3**) is accompanied by a prototropic shift within the diene system.

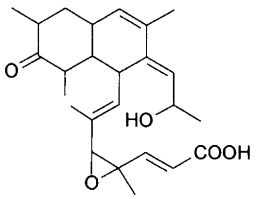

3

$^1H,^1H$ coupling patterns, supplemented with appropriate NOE-measurements, ascertained the identity of both the side-chains and the configurations at C-10, C-13, C-15, and C-16 of hamigerone and its dihydroanalogue. NOE correlations from H-8 to H-9, H-9′, and H-15 proved the former to be positioned equatorially and *cis* to H-15, whereas a marked NOE from H-2 to H-16 revealed their spatial proximity and hence that the *E*-configuration prevails at the C-3/C-4 double bond. Our data do not permit the assignment of configuration to C-2. Apart from this, we conclude that dihydrohamig-

erone is defined by structure **4** (or its mirror image), with the side-chain, R, represented by the formula shown, or its mirror image.

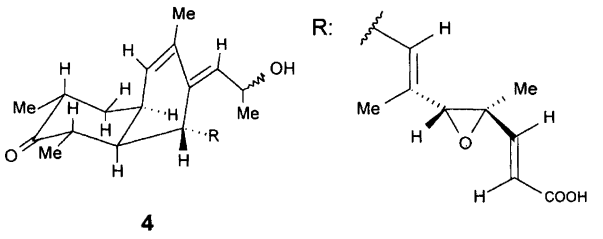

4

Biosynthesis. The long-chain substituted, bicyclic ketone structures, encountered in hamigerone and its dihydro congener, seem without obvious precedents within the large class of fungal metabolites; a fact that spurred our interest in their biosynthesis.

Shake flask cultures of *H. avellanea* were grown in the presence of variously ^{13}C-labelled precursors (Table 2). After seven days, the isotopically enriched hamigerone specimens were isolated and subjected to ^{13}C NMR analysis. The results, summarised in Table 2, clearly reveal that hamigerone derives, pleasingly straightforwardly, from ten acetate- and five methionine-derived C_1 units, as set out in the Scheme 1. Accordingly,

Table 2. Enrichment factors determined for hamigerone (**1**) derived from variously labelled precursors. Figures representing significant enrichments appear in bold typeface.

C	[1-^{13}C]Ac[a]	[2-^{13}C]Ac[a]	[*methyl*-^{13}C]Met[b]
1	0.9	**2.8**	1.0
2	**2.7**	0.6	1.0
3	0.8	**2.2**	1.1
4	**2.6**	1.0	1.2
5	0.7	**2.9**	1.0
6	—	—	**10.7**
7	**3.0**	0.7	0.9
8	0.7	**2.2**	0.9
9	**3.2**	0.9	1.0
10	0.8	**2.1**	1.0
11	—	—	**9.5**
12	**3.7**	0.9	1.1
13	0.8	**2.2**	1.0
14	—	—	**13.4**
15	**2.9**	0.8	1.0
16	0.8	**2.9**	1.0
17	**2.8**	0.8	1.0
18	0.9	**4.1**	1.0
19	—	—	**12.2**
20	**4.3**	0.7	0.9
21	0.8	**2.8**	0.9
22	—	—	**14.3**
23	**4.2**	0.7	1.0
24	0.8	**3.4**	1.0
25	**2.8**	0.7[c]	0.8[c]

[a] Spectra normalized to the average intensity for the signals corresponding to C-6, C-11, C-14, C-19 and C-22. [b] Spectra normalized to the intensity of the signal corresponding to C-1. [c] Intensity of signals based on integration (see the Experimental).

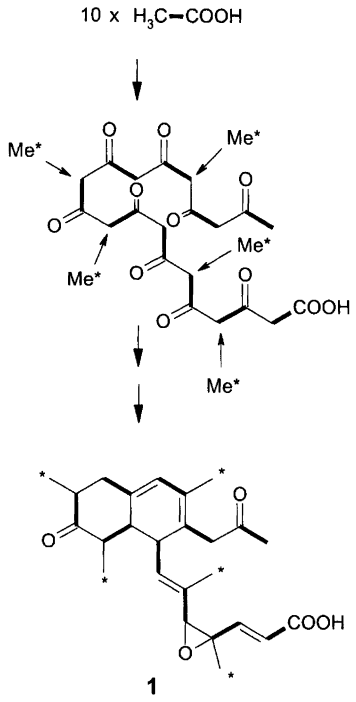

1

Scheme 1.

2D-INADEQUATE analysis of a hamigerone specimen, produced in the presence of [1,2-$^{13}C_2$]acetate, exhibited ^{13}C,^{13}C couplings between the pairs C1–C2, C3–C4, C5–C7, C8–C9, C10–C12, C13–C15, C16–C17, C18–C20, C21–C23, and C24–C25, corresponding to the incorporation of ten intact C_2-units. Though unproven, the *in vivo* route to dihydrohamigerone most likely follows the same pathway.

Biological activity and discussion

Experiments, conducted *in vitro* with the plant pathogenic fungi *P. oryzae* and *Venturia inaequalis* (Ascomycota) as test organisms, revealed a growth inhibitory activity of hamigerone comparable to that of commercial fungicides such as Prochloraz® and Bitertanol®, whereas dihydrohamigerone showed only marginal activity. When tested for its ability to protect rice plants against subsequent infection with *P. oryzae*, hamigerone proved far inferior to the commercial fungicides.

Apart from the ability to produce hamigerone and dihydrohamigerone, the fungus *H. avellanea* possesses a recorded capacity for synthesising other and structurally unrelated compounds, such as the potent, hypertensive cyclopentapeptides avellanins A and B,[1] and a substituted 2,3-bisformamido-1,4-diphenylbutadiene, devoid of notable antifungal activity, recently reported from our laboratories.[2]

Experimental

^{1}H and ^{13}C NMR data were acquired at 297 K on Bruker AC300P or AMX600 instruments. Chemical

shifts (δ) are in ppm, coupling constants (*J*) in Hz. EI mass spectra, at 70 eV ionisation potential, and high-resolution fast atom bombardment (HR-FAB) MS were performed on a JEOL AX505W instrument. EI MS are presented as *m/z* (% rel. int.). Growth inhibitory activity, *in vitro*, was assessed in agar diffusion assays as previously described.[3] CCC was performed on a PTR CCC-1000 (Pharma-Tech Research Corp, Baltimore) counter-current chromatograph equipped with a 320 ml column.

Isolation and purification of hamigerone (**1**) *and dihydrohamigerone* (**3**). The filtrate (12.5 l) from submerged fermentations of *H. avellanea* (CBS 501.94) conducted as previously described,[2] was passed through a column of XAD-1180 resin (1.3 l) over the course of 4 h. After being washed with water (1.3 l), the column was eluted stepwise with gradients of EtOH in H_2O [25:75 (1.3 l)→50:50 (1.3 l)→75:25 (1.3 l)→100:0 (0.4 l)] followed by elution with EtOH (2 l). The last eluate was evaporated to a syrupy residue (6.6 g).

The residue, divided into two halves, was applied to two silica gel columns (Merck Si60, 63–200 μm, 160 × 40 mm), equilibrated with heptane–EtOAc (9:1). Stepwise gradients of heptane–EtOAc–MeOH (fraction size 0.4 l)(9:1:0→1:1:0→0:1:0→0:3:1) were used as eluents, followed by a 0:1:1 elution. The latter, combined from the two columns, was evaporated to give an oily residue (850 mg).

Further purification involved chromatography, either on a silica gel column [Lichroprep Si60 Lobar B (Merck)], eluted over the course of 1 h, with a linear gradient from CH_2Cl_2 to CH_2Cl_2–MeOH (1:1) (flow rate 7.5 ml min^{-1}), or, alternatively, counter current chromatography (CCC) using the solvent system heptane–EtOAc–MeOH–H_2O (2:8:5:5) with the upper phase as the stationary phase. The column was rotated at 1000 rpm and eluted at a flow rate of 1.5 ml min^{-1}. Retention of the stationary phase was approximately 40%. In both cases the effluent was monitored by UV absorption at 240 and 280 nm. A highly purified mixture of hamigerone (**1**) and dihydrohamigerone (**3**) resulted (530 mg). Though varying somewhat from one fermentation to another, a typical ratio of **1**:**3** was 10:1.

Final purification was achieved by reversed phase HPLC (Dupont ODS (10 μm), 150 × 20 mm column), eluting isocratically with 55% aqueous acetonitrile (0.05% H_3PO_4), flow rate: 10 ml min^{-1}; $t_R{}^3$ 8.4 min and $t_R{}^1$ 9.5 min. Fractions containing only **1**, or **3**, were separately extracted twice with CH_2Cl_2 (1 vol.). The organic phases were washed with water (1 vol.), dried, and freed of solvent to yield **1** and **3** as colourless glasses.

Hamigerone (**1**): NMR data: see Table 1. EI-MS: 412 (6, M^+), 297 (42), 255 (83), 241 (100), 240 (96), 211 (67), 201 (91), 197 (74), 184 (72), 171 (80), and 157 (77). HR-FABMS: found 411.2160, calc. for $C_{25}H_{31}O_5$ ($M-1$) 411.2171. $[\alpha]_D{}^{22} = -345°$ ($c = 0.4$, MeOH). IR (KBr): 3427, 2971, 2932, 1707, 1651, 1453, 1418, 1380, 1356, 1307, 1282, 1158, and 982 cm^{-1}. UV (H_2O–MeCN 1:1): 280 nm.

Dihydrohamigerone (**3**): NMR data: see Table 1. HR-FABMS: found 413.2325, calc. for $C_{25}H_{33}O_5$ ($M-1$) 413.2328; $[\alpha]_D{}^{22} = -7°$ ($c = 0.3$, MeOH). UV (H_2O–MeCN 1:1): 240 nm.

Feeding experiments. Feeding experiments were performed in duplicate using [1-^{13}C]acetate, [2-^{13}C]acetate, [1,2-$^{13}C_2$]acetate, and (2*S*)-[*methyl*-^{13}C]methionine. Two portions of the precursors dissolved in water (2 × 125 mg of acetate and 2 × 10 mg of methionine) were separately added, via syringes equipped with sterile filters, to cultures grown in 500 ml Erlenmeyer flasks each containing 100 ml of growth medium as described previously[2] 56 and 104 h after inoculation. The fermentation was continued for 170 h. The whole fermentation broth was extracted with EtOAc (100 ml) with vigorous stirring followed by phase separation facilitated by centrifugation. The aqueous phase was extracted again with 100 and 50 ml portions of EtOAc. The combined organic extracts were dried (freezing and removal of the separated ice) and the solvent evaporated off *in vacuo*. Labelled specimens of **1** were obtained by preparative silica gel TLC and reversed phase HPLC as described above. An untreated shake flask was processed identically to yield an unlabelled specimen of **1** serving as a natural abundance reference for the ^{13}C NMR analyses.

Labelled products were dissolved in $CDCl_3$ (600 μl) and ^{13}C NMR spectra acquired (15 000–20 000 scans with 2 s repetition delay). Enrichment factors (EF) for the labelled materials (Table 2) were determined as the ratio between relative peak heights (normalised to the average intensity of C-6, C-11, C-14, C-19, and C-22 for the acetate experiments, and to the intensity of C-1 in the methionine experiment) observed for the enriched material, and the relative peak heights observed in the natural abundance spectrum. The linewidth, and thus the peak height, of the signal corresponding to C-25 (carboxy group) varied and the enrichment factor for C-25 was assessed by comparing the integral of the C-25 signal with that of the signal corresponding to C-23. The 2D-INADEQUATE spectrum of **1** derived from doubly labelled acetate was optimised for $^1J_{CC} = 50$ Hz.

Acknowledgments. We thank Dr. Svend Ludvigsen for recording the 600 MHz NOESY-spectrum.

References

1. Yamazaki, M., Horie, Y., Bae, K., Maebayashi, Y., Jisai, Y. and Fujimoto, H. *Chem. Pharm. Bull. 35* (1987) 2122.
2. Breinholt, J., Kjœr, A., Olsen, C. E. and Rassing, B. R. *Acta Chem. Scand. 50* (1996) 643.
3. Berova, N., Breinholt, J., Jensen, G. W., Kjœr, A., Lo, L.-C., Nakanishi, K., Nielsen, R. I., Olsen, C. E., Pedersen, C. and Stidsen, C. E. *Acta Chem. Scand. 48* (1994) 240.

Received April 4, 1997.